EM Developments for a Radio Astronomy Polarimeter: The QUIJOTE Experiment

E. Artal, J.L. Cano, A. Mediavilla, E. Villa, B. Aja, L. de la Fuente, J. Cagigas[1]

***Abstract* – A comparison between simulated and measured results in different subsystems of a radio astronomy polarimeter receiver at 26-36 GHz band is presented. This comparison underlines the importance of careful simulation with different electromagnetic software tools in order to predict the receiver behavior. The receiver obtains three (*Q*, *U* and *I*) Stokes parameters simultaneously.**

1 INTRODUCTION

In radio astronomy there is an increasing interest in the measurement of Cosmic Microwave Background (CMB) polarization, in order to increase the knowledge of the Universe birth obtained with previous space missions such as COBE [1], WMAP [2] or Planck [3].

The QUIJOTE experiment [4] is a radio astronomy project aimed to characterize the polarization of the CMB and other galactic and extragalactic emissions. Its second phase, currently under development, is about a new instrument with 31 pixels or receivers, all in the 26 to 36 GHz band. The configuration of each pixel is presented in Fig. 1.

Many different subsystems in the receiver configuration shown in Fig. 1 are carefully simulated using electromagnetic (EM) tools. The feedhorn, polarizer and orthomode transducer (OMT) are designed and optimized using a mode matching tool such as µWave Wizard™ [5], and then their performance is checked using a full-3D EM software such as CST Microwave Studio® [6]. The same strategy is followed with the power-splitters and the 90º-phase shifter in the Back-End Module (BEM) designed on the WR28 waveguide. Planar structure circuits such as phase switches, filters, 180º hybrids and detectors are designed using a 2.5D EM tool such as ADS Momentum [7] and checked with CST. The use of different EM tools increase the confidence in the simulated results and therefore it reduces the number of iterations during the design process.

2 SUBSYSTEMS DESIGN

2.1 Horn Antenna

The antenna is a corrugated horn. The design starts with the throat (narrower section). An initial circular section with diameter d = 8 mm assures a good matching at the beginning of the bandwidth without enabling the propagation of higher order modes. After this constant section, just a few corrugations with increasing diameters are enough to define the matching and cross-polarization performance in the whole band. These few corrugations are optimized in their thickness and depth to achieve the desired performance. The optimization strategy for this section was focused in the cross-polarization parameter since it is the most important characteristic for an antenna intended for polarimetry.

The remaining corrugations have constant thickness and depth but increasing diameters. This section is optimized for achieving enough gain and the desired radiation pattern. Due to mechanical constraints, this section is divided for manufaturing into two additional parts.

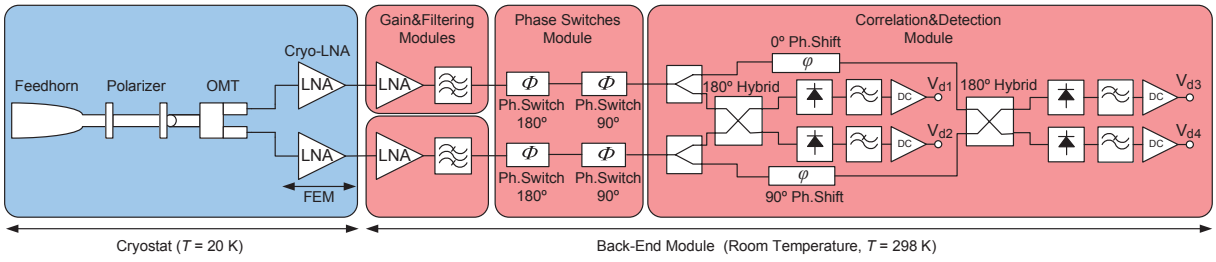

Figure 1. Configuration of each receiver in the QUIJOTE second phase.

Figure 2 shows a cross-section of the horn. The results obtained from the simulations are presented in Fig. 3, together with those obtained from measurements in an anechoic chamber.

[1] Departamento de Ingeniería de Comunicaciones, Universidad de Cantabria, Plaza de la Ciencia, 39005 Santander, Spain, e-mail: eduardo.artal@unican.es, tel.: +34 942 201397, fax: +34 942 201488.

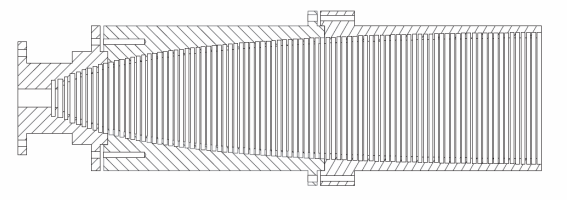

Figure 2. Cross-section of the horn antenna.

Measured cross-polarization in Fig. 3 is limited by the noise floor in the test setup.

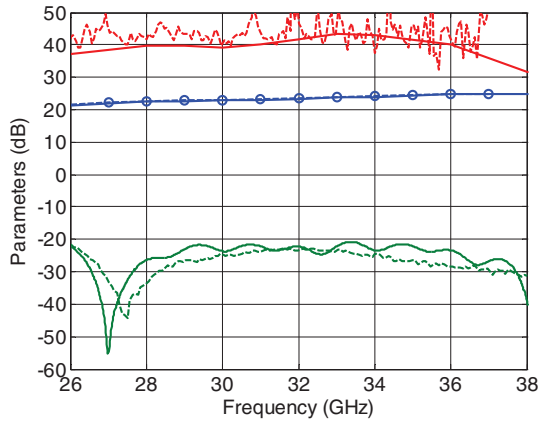

Figure 3. Simulated (solid lines) and measured (dashed lines) horn antenna performances: return loss (green), directivity (blue line with circles), simulated gain (blue) and cross-polarization (red).

2.2 Polarizer

The polarizer is a square waveguide with a ridge in each internal wall. It acts like a 90º phase shifter between the two propagated modes. If the polarizer is placed in front of the OMT rotated 45º then the assembly works as a septum polarizer. The polarizer, Fig 4, is a frequency scaled and mechanically improved version of the component presented in [8].

Measured results are presented in Fig. 5 compared with simulations. Return loss results along y-axis are not shown for clarity, being similar to x-axis return loss. Polarizer insertion losses are around 0.18 dB.

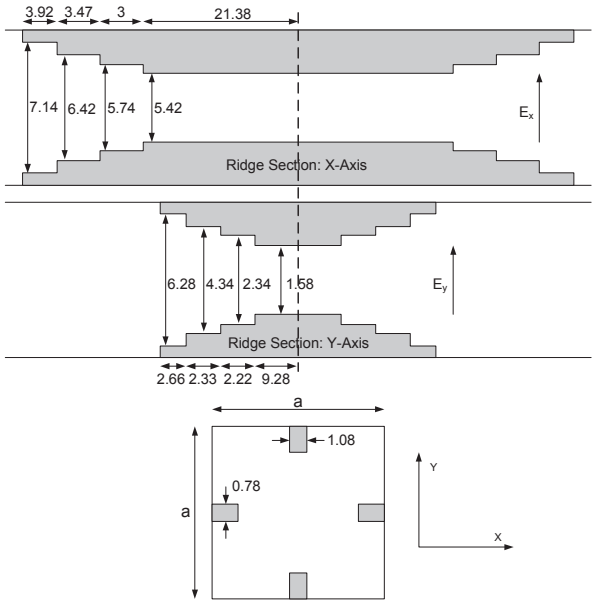

Figure 4. Cross-sections and front-view of the polarizer with all the dimensions. Units in mm.

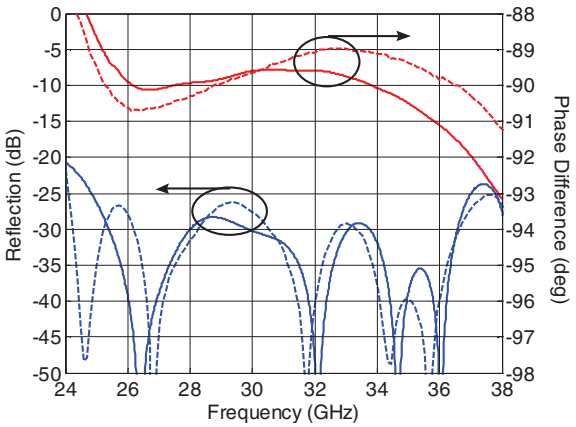

Figure 5. Simulated (solid lines) and measured (dashed lines) performance of the polarizer: return loss along x-axis and phase difference between outputs.

2.3 Orthomode Transducer (OMT)

The OMT separates the orthogonal components of the incoming signal. OMT design is divided in three parts: turnstile junction, E-plane bends and power combiner. These parts are simulated and optimized separately and finally put together. Due to the system requirements, both rectangular waveguide outputs need to be in-phase. This OMT is an improved version of the component presented in [9]. Comparison of simulation and test results are in Fig. 6. Measured insertion losses are around 0.15 dB and phase difference between both branches is 1º±1º across the band.

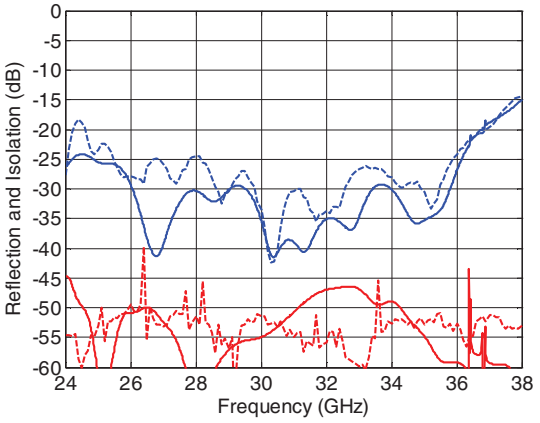

Figure 6. Simulated (solid line) and measured (dashed line) performance of the OMT: return loss (blue) at rectangular port, and isolation between rectangular ports (red).

2.4 Planar Structure Circuits

2.4.1 Phase Switches Module

The Phase Switches Module modulates the state of the receiver by generating sixteen phase states. The module consists of two identical branches, each one with two cascaded 180º and 90º phase switches. Their combination introduces four states per branch.

The design of the 180º phase switch is based on uniplanar technology. The phase difference is introduced by feeding a coplanar waveguide structure by opposite gaps generating out-of-phase electromagnetic fields [10]. Phase difference error is lower than 2 degress in the band.

The 90º phase switch is based on planar structures combined by a single pole double throw switch [11]. Phase and amplitude imbalance results are depicted in Fig. 7.

2.4.2 Band-Pass Filter

The bandwidth of the full receiver is defined by a microstrip band-pass filter on Alumina substrate (ε_r = 9.9 and h = 254 µm) [12]. Measured insertion loss is around 0.8 dB and return losses are better than 10 dB in the whole band.

2.4.3 180º Hybrid

Stokes parameters calculation requires signals correlation, carried out using two 180º hybrids prior signal detection. The hybrid is in Fig. 8.

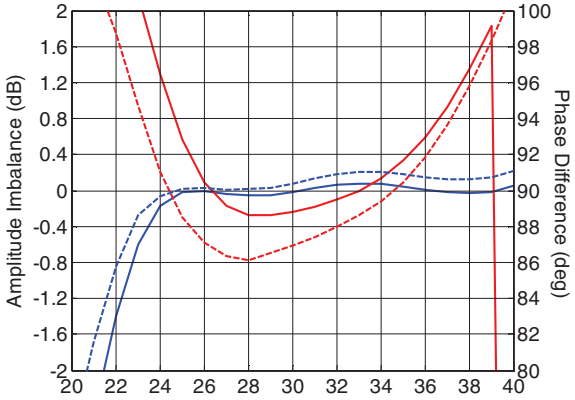

Figure 7. Simulated (solid line) and measured (dashed line) performance of the 90º phase switch: amplitude imbalance (blue), and phase difference (red).

Figure 8. Prototype of 180º hybrid. Reference planes for measurement and simulation are marked with red lines.

It is a three sections rat-race hybrid to increase its bandwidth [13]. Coplanar to microstrip transitions are used for experimental tests. Phase imbalance is lower than 2 degrees.

2.4.4 Detector

It is a microstrip Schottky zero-bias diode detector, shown in Fig. 9. Thin film distributed resistors, based on TaN resistive layer of 20 Ohm/sq, are used to flatten the frequency response and to achieve a good input matching. Measured return loss is around 12 dB. Average detector sensitivity is 1300 mV/mW in the band. There is a coplanar-to-microstrip transition for testing.

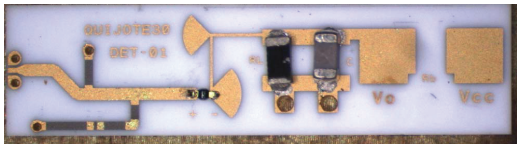

Figure 9. Schottky diode detector.

3 RECEIVER OPERATION

With the receiver shown in Fig. 1, at the OMT outputs there are two signals corresponding with the two components of the incoming radiation in the circular basis: A and B.

$$A = \frac{1}{\sqrt{2}}(E_x + jE_y) \quad (1)$$

$$B = \frac{1}{\sqrt{2}}(E_x - jE_y) \quad (2)$$

Where E_x and E_y are the electric-field cartesian components of the sky emission. Considering a first state in the phase switch module with $\Delta\varphi = 0º$ of phase difference between both branches, then the detected voltages are used to calculate the Stokes parameters as stated in (3)-(5) [14], [15].

$$V_{d1} - V_{d2} = 4\,\mathrm{Re}\left\langle AB^* \right\rangle = Q \quad (3)$$

$$V_{d3} - V_{d4} = 4\,\mathrm{Im}\left\langle AB^* \right\rangle = U \quad (4)$$

$$V_{d1} + V_{d2} = V_{d3} + V_{d4} = \left\langle |A|^2 + |B|^2 \right\rangle = I \quad (5)$$

There are sixteen different states of the Phase Switches. Stokes parameters are calculated from different states to minimize the systematics errors.

4 CONCLUSIONS

A 26-36 GHz polarimeter for the QUIJOTE Experiment is presented. Each subsystem behaviour is shown comparing simulation and test results. The similarity between both results stresses the importance of EM simulation to predict the real behaviour. The use of different simulators is advisable to detect discrepancies.

Acknowledgments

Authors would like to thank Eva Cuerno and Ana R. Pérez for their careful work during the assembly.

This work has been funded by the Ministerio de Ciencia e Innovación (Spain) under Astronomy and Astrophysics research programme, reference AYA2010-21766-C03-03.

References

[1] Cosmic Background Explorer (COBE) http://lambda.gsfc.nasa.gov/product/cobe/

[2] Wilkinson Microwave Anisotropy Probe http://lambda.gsfc.nasa.gov/product/map/current/

[3] Planck Mission webpage (ESA) http://www.esa.int/Our_Activities/Space_Science/Planck

[4] QUIJOTE Experiment http://www.iac.es/proyecto/cmb/pages/en/home-cmb.php

[5] µWave Wizard™, Mician GmbH, Bremen, Germany. http://www.mician.com

[6] CST Microwave Studio, Computer Simulation Technology AG., MA, USA. http://www.cst.com

[7] ADS Momentum, Agilent Technologies, Inc., CA, USA. http://www.home.agilent.com

[8] A. Tribak, A. Mediavilla, J. L Cano, M. Boussouis, and K. Cepero, "Ultra-Broadband Low Axial Ratio Corrugated Quad-Ridge Polarizer", Proc. 39th European Microwave Conf. (39th EuMC), Roma, Italy, Oct. 2009, pp. 73-76.

[9] J. L. Cano, A. Tribak, R. Hoyland, A. Mediavilla, and E. Artal, "Full Band Waveguide Turnstile Junction Orthomode Transducer with Phase Matched Outputs", Int. Jrnl. RF and Microwave CAE, vol. 20, no. 3, May 2010, pp. 333-341.

[10] E. Villa, B. Aja, L. de la Fuente and E. Artal, "Wideband uniplanar 180º phase switch," Electronics Letters, Vol. 45, Issue 11, May 2009.

[11] E. Villa, L. de la Fuente, J. Cagigas, B. Aja, and E. Artal, "Wideband Ka-band 90º phase switch for radio astronomy," Electron. Lett., Vol. 49, Issue 5, Feb. 2013.

[12] J. L. Cano, B. Aja, E. Villa, L. de la Fuente, and E. Artal, "Broadband Back-End Module for Radio-Astronomy Applications in the Ka-Band", Proc. 38th European Microwave Conference, Oct. 2008, Amsterdam. pp. 1113-1116.

[13] Muraguchi, T. Yukitake, and Y. Naito, "Optimum design of 3 dB branch-line couplers using microstrip lines," *IEEE Trans. Microw. Theory Tech.*, vol. MTT-31, no. 8, pp. 674–678, Aug. 1983.

[14] Stokes parameters definition in Wikipedia: http://en.wikipedia.org/wiki/Stokes_parameters

[15] G. Virone, R. Tascone, M. Baralis, A. Olivieri, O. A. Peverini, and R. Orta, "Five-Level Waveguide Correlation Unit for Astrophysical Polarimetric Measurements", IEEE Trans. Microwave Theory and Tech., vol. 55, no. 2, February 2007, pp. 309-317.